

Proc. Ito Int. Research Center Symp. "Perspectives of the Physics of Nuclear Structure" JPS Conf. Proc. 23, 012014 (2018) https://doi.org/10.7566/JPSCP.23.012014

Structure of exotic nuclei based on nuclear force

Naofumi Tsunoda¹, Takaharu Otsuka^{2,3,4,5}, Noritaka Shimizu¹, Morten Hjorth-Jensen^{6,7}, Kazuo Takayanagi⁸ and Toshio Suzuki⁹

USA

E-mail: tsunoda@cns.s.u-tokyo.ac.jp

(Received April 1, 2018)

We present a novel method which enables us to perform shell-model calculations with several major shells (e.g. sd+pf). We present various observables, giving the first shell-model description for the island of inversion without two-body matrix elements fitted to experiment. Multiple particle-hole excitations over the N=20 magic gap is shown to be crucial for the structure of ^{30,31}Mg, as an example.

KEYWORDS: shell model, exotic nuclei, perturbation theory, nuclear force

1. Introduction

Exotic nuclei are located far from the β -stability line on the Segré chart, exhibiting very short life times, mainly due to an unbalanced ratio of proton (Z) and neutron (N) numbers. They differ remarkably from stable nuclei and their properties provide us new insights in understanding atomic nuclei and nuclear forces.

The nuclear shell model(SM) and shell-model calculations provide a unified and successful description of both stable and exotic nuclei. Shell-model calculations handle the nuclear forces in terms of single-particle energies (SPEs) and two-body matrix elements (TBMEs), which is often referred as effective interaction.

Obviously, for most of nuclei in the Segré chart, direct solution of full many-body problem cannot be obtained. Then we apply so-called model space, where necessary degrees of freedom for the specific problem are included. The ultimate goal of this direction is, of course, that effective interactions are derived from nuclear force for all possible model space so that we can calculate all the nuclei in the Segré chart, including stable and unstable exotic nuclei. Theoretical framework has been developing so far in this line.

In early days, effective interactions were determined empirically to reproduce selected experimental observables. A well-known example is the effective interaction for *p*-shell nuclei by Cohen and Kurath [1]. A breakthrough towards more microscopically-derived TBMEs was achieved by Kuo

¹ Center for Nuclear Study, the University of Tokyo, 7-3-1 Hongo, Bunkyo-ku, Tokyo, Japan

² Department of Physics and Center for Nuclear Study, the University of Tokyo, 7-3-1 Hongo, Bunkyo-ku, Tokyo, Japan

³ RIKEN Nishina Center, 2-1 Hirosawa, Wako, Saitama 351-0198, Japan

⁴ National Superconducting Cyclotron Laboratory, Michigan State University, East Lansing, Michigan, 48824, USA

⁵ Instituut voor Kernen Stralingsfysica, Katholieke Universiteit Leuven, B-3001 Leuven, Belgium

⁶ Department of Physics and Astronomy, Michigan State University, East Lansing, Michigan, 48824, USA

⁷ Department of Physics, University of Oslo, N-0316 Oslo, Norway ⁸ Department of Physics, Sophia University, 7-1 Kioi-cho, Chiyoda-ku, Tokyo 102, Japan

⁹ Department of Physics, College of Humanities and Sciences, Nihon University, Sakurajosui 3, Setagaya-ku, Tokyo 156-8550, Japan

and Brown for *sd*-shell nuclei [2]. Although basic features of the nucleon-nucleon (*NN*) force for the SM calculation are included in these effective interactions, empirical adjustments of TBMEs were needed in order to reproduce various observables [3].

These effective interactions were all derived for a Hilbert space represented by one major oscillator shell. This is partly because computer power at that time is not enough, partly because microscopic theory is not ready, to handle more than one major shell.

As experimental techniques and computational capability had been developed, our interests moved to exotic nuclei both from experimental side and theoretical side. Then, some new features and phenomena arise. A notable example is significant particle-hole excitations across the major shell gap, for example, in Z=8-14 neutron-rich exotic nuclei [4–6]. To describe many of these phenomena naturally, it is required that we handle more than one major shell, which means we need the technique of large-scale SM calculation and a new microscopic theory.

Deriving SM effective Hamiltonians is a challenge to nuclear theory. Several attempts have been made recently in this direction while the issue of two major shells is still unsettled.

In the proceedings, we will first present the novel method called Extended Kuo-Krenciglowa method (EKK) to derive the effective interaction within more than one major shell. Then, we will derive SM interaction for the model space consisting of the sd and pf shells based on the so-called Extended Kuo-Krenciglowa (EKK) method. Secondly, we apply this interaction to our studies of exotic neutron-rich Ne, Mg and Si isotopes. These are nuclei in and around the so-called "island of inversion", where the degrees of freedom of sd and pf shells are essential. Three-nucleon forces (3NFs) are also included since they play an important role in reproducing basic nuclear properties.

2. Extended Kuo-Krenciglowa method

In this section we will propose a new method called Extended Kuo-Kurenciglowa (EKK) method. This method is designed to derive effective interactions in non-degenerate model space, in this case, model space represented by more than one major oscillator shell [7–9]. Many-body perturbation theory (MBPT) has been the model of choice for deriving effective interactions for the shell model, see for example Refs. [10,11]. Conventional MBPTs, such as Kuo-Kurenciglowa (KK) method [10], are constructed for degenerate single-particle states in the model space. Let us introduce KK method first.

Suppose we describe a quantum system by the following Hamiltonian

$$H = H_0 + V, (1)$$

where H_0 is the unperturbed Hamiltonian and V is the perturbation. In a Hilbert space of dimension D, we can write down the many-body Schrödinger equation as

$$H|\Psi_{\lambda}\rangle = E_{\lambda}|\Psi_{\lambda}\rangle, \quad \lambda = 1, \cdots, D.$$
 (2)

In shell-model calculations, however, the dimension D of the Hamiltonian matrix increases exponentially with the particle number, limiting thereby the applicability of direct diagonalization procedures to the solution to Eq. (2).

In this situation, we introduce a P-space (model space) of a tractable dimension d that is a subspace of the large Hilbert space of dimension D. Correspondingly, we define the projection operator P onto the P-space, and Q = 1 - P onto its complement. We require that the projection operators P and Q commute with the unperturbed Hamiltonian H_0 ,

$$[P, H_0] = [Q, H_0] = 0.$$
 (3)

We start our explanation by introducing an energy-dependent effective Hamiltonian. By use of the

projection operators P and Q, we can express Eq. (2) in the following partitioned form $(\lambda = 1, \dots, D)$:

$$\begin{pmatrix} PHP & PVQ \\ QVP & QHQ \end{pmatrix} \begin{pmatrix} |\phi_{\lambda}\rangle \\ |\Psi_{\lambda}\rangle - |\phi_{\lambda}\rangle \end{pmatrix} = E_{\lambda} \begin{pmatrix} |\phi_{\lambda}\rangle \\ |\Psi_{\lambda}\rangle - |\phi_{\lambda}\rangle \end{pmatrix}, \tag{4}$$

where $|\phi_{\lambda}\rangle = P|\Psi_{\lambda}\rangle$ is the projection of the true eigenstate $|\Psi_{\lambda}\rangle$ onto the *P*-space. Then we can solve Eq. (4) for $|\phi_{\lambda}\rangle$ as

$$H_{\rm BH}(E_{\lambda})|\phi_{\lambda}\rangle = E_{\lambda}|\phi_{\lambda}\rangle, \quad \lambda = 1, \cdots, D.$$
 (5)

where we have introduced the following Bloch-Horowitz effective Hamiltonian $H_{\rm BH}$ defined purely in the P-space

$$H_{\rm BH}(E) = PHP - PVQ \frac{1}{E - OHO} QVP. \tag{6}$$

Note that Eq. (5) requires a self-consistent solution, because $H_{BH}(E_{\lambda})$ depends on the eigenenergy E_{λ} . This is not a desirable property for the shell-model calculation.

To remove this unwanted energy dependence, following infinite series can be utilized,

$$V_{\text{eff}}^{(n)} = \hat{Q}(\epsilon_0) + \sum_{k=1}^{\infty} \hat{Q}_k(\epsilon_0) \{V_{\text{eff}}^{(n-1)}\}^k, \tag{7}$$

where we have defined \hat{Q} -box and its derivatives as follows:

$$\hat{Q}(E) = PVP + PVQ \frac{1}{E - QHQ} QVP, \quad \hat{Q}_k(E) = \frac{1}{k!} \frac{d^k \hat{Q}(E)}{dE^k}.$$
 (8)

In the limit of $n \to \infty$, Eq. (7) gives $V_{\rm eff} = V_{\rm eff}^{(\infty)}$, if the iteration converges, see Ref. [11] for more in detail. This can be intuitively understood with an analogy of Taylor expansion of an function

$$f(x) = f(\epsilon_0) + \sum_{k=1}^{\infty} \frac{1}{k!} f^{(k)}(\epsilon_0) \cdot x^k.$$
 (9)

We stress here that the above KK method can only be applied, by construction, to a system with a degenerate unperturbed model space that satisfies $PH_0P = \epsilon_0P$. It cannot be applied, for instance, to obtain the effective interaction for the model space composed of sd and pf-shells.

EKK method is invented to overcome this difficulty. Detailed derivation of EKK method is written in Ref. [9], but in this proceedings, we will explain intuitively following the same analogy of Taylor expansion above. In EKK method, we utilize following division of the same Hamiltonian,

$$H = H'_0 + V'$$

$$= \begin{pmatrix} E & 0 \\ 0 & OH_0O \end{pmatrix} + \begin{pmatrix} P\tilde{H}P & PVQ \\ OVP & OVO \end{pmatrix}, \tag{10}$$

where $\tilde{H} \equiv H - E$. Then, because of the property of Taylor expansion, we can change the origin of expansion from ϵ_0 to any value (in this case E) and we get the following:

$$\tilde{H}_{\text{eff}}^{(n)} = \tilde{H}_{\text{BH}}(E) + \sum_{k=1}^{\infty} \hat{Q}_k(E) \{ \tilde{H}_{\text{eff}}^{(n-1)} \}^k, \tag{11}$$

where tilde exhibits subtract E, which is the same manner as \tilde{H} . With this method, we do not need to set our P-space to degenerate one. Therefore, we can derive effective interaction for more than one major shell, for example, sdpf-shell.

3. Numerical results and comparisons to experimental data

In this section, we will present the numerical results of the application of the EKK method to the nuclei located into "island of inversion", including comparisons to latest experimental findings (see for example Ref. [12], more in detail). By utilizing EKK method, we derived a effective interaction for sdpf-shell. We added effective two-body force derived from Fujita-Miyazawa three-body force with its strength given by a standard π -N- Δ coupling [14, 15]. We call this new interaction as EEdf1 interaction hereafter. Then, we calculated Z = 8 - 14 isotopes with EEdf1 interaction to see if we can describe the properties of island of inversion.

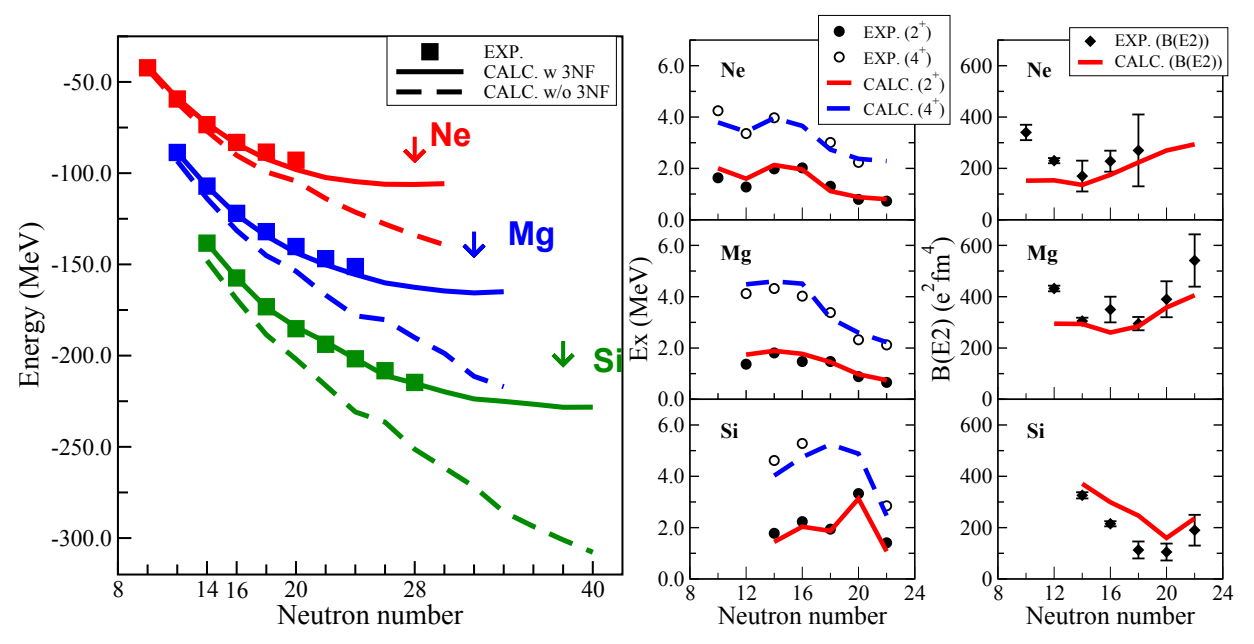


Fig. 1. (Left) Ground state energies of Ne, Mg, Si isotopes. (Middle) Energies of first excited 2⁺ and 4⁺ states and (Right) B(E2) values of Ne, Mg, Si isotopes.

Figure 1 shows various observables of Ne, Mg and Si isotopes. Left figure indicates the ground state energies are well reproduced when 3NF effects are included. It is also worth noticing that the repulsion due to the 3NF grows as *N* increases in all the isotopic chains. This is consistent with earlier studies [15]. We point out that this repulsion becomes stronger also as *Z* increases, suggesting that the present 3NF contribution is repulsive also in the proton-neutron channel. We also present predictions for the drip lines by arrows.

Middle figure shows the first excited 2^+ and 4^+ energies. Experimental levels are well reproduced by the present calculation, including both gradual and steep changes as a function of N. Most importantly, the low excitation energy of the 2^+_1 levels in 30 Ne and 32 Mg indicates that these nuclei are strongly deformed and that sd-to-pf particle-hole (ph) excitations over the N=20 gap occur significantly. In contrast, the higher-lying 2^+_1 level of 34 Si suggests weaker degrees of ph excitations. Right figure shows B(E2: $0^+_1 \rightarrow 2^+_1$) values. With effective charges, $(e_p, e_n) = (1.25, 0.25)e$,

Right figure shows B(E2: $0_1^+ \rightarrow 2_1^+$) values. With effective charges, $(e_p, e_n) = (1.25, 0.25)e$, calculated B(E2) values exhibit systematic behaviors in agreement with experiment. This agreement is, however, not as good as that obtained for the energy levels. This probably indicates the need to derive E2 operator using the same microscopic theory. While the N = 20 shell closure in Si isotopes is evident also in B(E2) systematics, the B(E2) values of Ne and Mg isotopes are larger at N = 20 than at N = 18, a feature which is consistent with growing deformation seen in the 2_1^+ level.

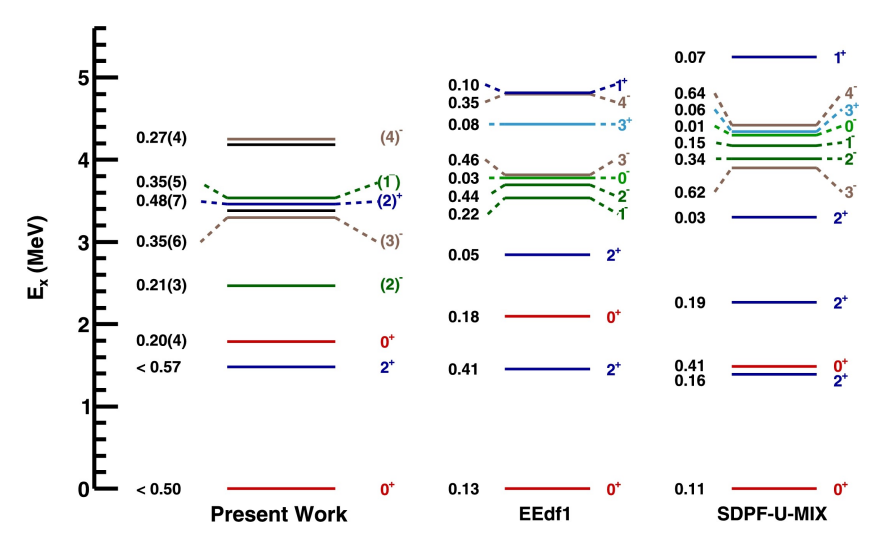


Fig. 2. Experimental and theoretical level scheme of ³⁰Mg. Numbers attached to the levels are spectroscopic factor of knockout reaction from ground state of ³¹Mg. This figure is taken from Ref. [13]

Next, we move to the comparison to latest experiment. Figure 2 shows the level schemes of 30 Mg [13]. This nuclei is considered to be located at the west coast of the "island of inversion". Therefore, the properties of the wavefunction are of great interest. This experiment is a knockout reaction from ground state of 31 Mg. With this experiment the spins, parities and spectroscopic factors are deduced. Two different theoretical calculations are shown for the reference, one of which is done by our EEdf1 interaction. The other is sdpf-U-mix interaction [16], which is an extension of sdpf-U interaction [17], allowing the np - nh excitation across the N = 20 gap. The sdpf-U is one of the successful interactions to reproduce the experimental data by fitting the TBMEs. With both interaction, 31 Mg is intruder character, but the details are different. SDPF-U-MIX wave function consists of 90% of the 2p - 2h, while in the case of EEdf1, 66% of 2p - 2h and 29% of 4p - 4h. In short, the wavefunction of EEdf1 includes more particle-hole excitation across the N = 20 gap. This tendency also seen for the other isotopes [12]. Looking at Fig. 2, both interaction reproduced experimental 3 lowest levels fairly well. This difference appears to the spectroscopic factors. In EEdf1, spectroscopic factor of 0^+_2 is smaller than 2^+_1 , whereas in sdpf-U-mix the situation is the opposite. Experimental data of spectroscopic factor seems to support our calculation.

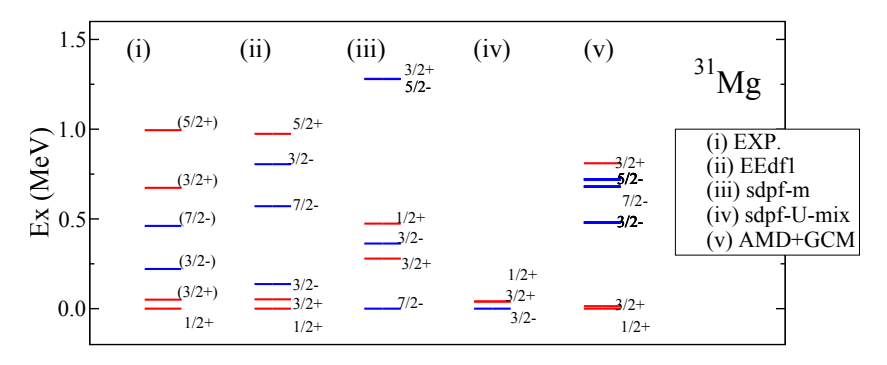


Fig. 3. Experimental and theoretical level scheme of ³¹Mg.

Figure 3 shows another comparison to experimental data. Since ³⁰Mg is on the boarder of the

"island of inversion", 31 Mg is located inside. Then, it is known that positive parity states and negative parity states are seen as the low-lying states. Our EEdf1 interaction reproduces the experimental level scheme well, while other empirical interactions do not. This supports our wavefunction which has large fraction of 2p-2h and 4p-4h configurations. The reason why empirical calculations do not reproduce the experimental data might simply be lack of experimental information when the fitting of TBMEs is executed. Especially since the experimental data of exotic nuclei are less abundant than stable nuclei, it is difficult to fix the inter-shell TBMEs (in this case, sd-pf shell TBMEs) from the experimental observations. The advantage of EKK method is that such fitting is not necessary and one can avoid those difficulties. More discussions and detailed comparisons to latest experimental data will be presented in Ref. [18].

4. Conclusion

First we presented a EKK method, which enables us to derive the effective interaction for the shell model for more than one major shell. The essence of EKK method is explained by an analogy to Taylor expansion. We calculated the effective interaction for sdpf-shell, which is named as EEdf1 interaction. Then, we presented numerical results of EEdf1 interaction and some comparison to experimental data. Ground state energies, energies of first excited 2^+ and 4^+ states and B(E2) values of even-even nuclei and inside and near the "island of inversion" are well reproduced. It is a characteristic feature of EEdf1 that its wavefunction exhibits large fraction of np - nh excitation across the N = 20 shell gap. Detailed comparison to experimental data of 30 Mg and 31 Mg support our wavefunction.

5. Acknowledgments

We thank Dr. Y. Utsuno for useful discussions. The Lanczos shell-model calculation is performed with the code "KSHELL" [19]. This work was supported in part by Grants-in-Aid for Scientific Research (23244049,15K05090). It was supported in part by HPCI Strategic Program (hp140210,hp150224), in part by MEXT and JICFuS as a priority issue (Elucidation of the fundamental laws and evolution of the universe) to be tackled by using Post 'K' Computer, and also by CNS-RIKEN joint project for large-scale nuclear structure calculations.

References

- [1] S. Cohen and D. Kurath, Nucl. Phys. 73, 1 (1965).
- [2] T. T. S. Kuo and G. E. Brown, Nucl. Phys. 85, 40 (1966).
- [3] B. A. Brown, W. A. Richter, R. E. Julies, and B. H. Wildenthal, Annals of Physics 182, 191 (1988).
- [4] O. Sorlin and M. G. Porquet, Prog. Part. Nucl. Phys. 61, 602 (2008).
- [5] E. Caurier, G. Martínez-Pinedo, F. Nowacki, A. Poves and A. P. Zuker, Rev. Mod. Phys. 77, 427 (2005).
- [6] Y. Utsuno, T. Otsuka, T. Mizusaki, and M. Honma, Phys. Rev. C 60, 054315 (1999).
- [7] K. Takayanagi, Nucl. Phys. A 852, **61** (2011).
- [8] K. Takayanagi, Nucl. Phys. A 864, **91** (2011).
- [9] N. Tsunoda, K. Takayanagi, M. Hjorth-Jensen, and T. Otsuka, Phys. Rev. C 89, 024313 (2014).
- [10] T. T. S. Kuo, S. Y. Lee, and K. F. Ratcliff, Nucl. Phys. A 176, 65 (1971).
- [11] M. Hjorth-Jensen, T. T. S. Kuo, and E. Osnes, Phys. Rep. 261, 125 (1995).
- [12] N. Tsunoda et al., Phys. Rev. C 95, 021304 (2017).
- [13] B. Fernndez-Domnguez et al., Phys. Lett. B 779, 124 (2018).
- [14] A. M. Green, Rept. Prog. Phys. 39, 1109 (1976).
- [15] T. Otsuka et al., Phys. Rev. Lett. 105, 032501 (2010).
- [16] E. Caurier et al., Phys. Rev. C 90, 014302 (2014).
- [17] F. Nowacki and A. Poves, Phys. Rev. C 79, 014310 (2009).
- [18] H. Nishibata et al., submitted (2018).
- [19] N. Shimizu, arXiv:1310.5431v1 [nucl-th] (2013).